AD-A274 418

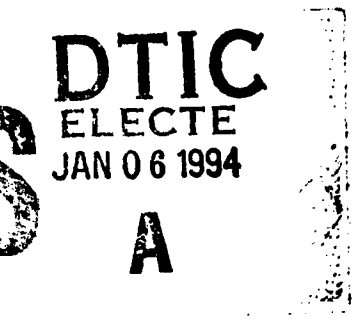

Quarterly Progress Report

September 1, 1993 to November 30, 1993

Visible Light Emitting Materials and Injection Devices

ONR/ARPA URI

Grant Number N00014-92-J-1895

Prepared by:

Paul H. Holloway
Department of Materials Science and Engineering
University of Florida
P.O. Box 116400
Gainesville, FL 32611
Ph: 904/392-6664; FAX 904/392-4911
E-Mail: Internet-PHOLL@MSE.UFL.EDU

This document has been approved for public release and sale; its distribution is unlimited.

Participants:
University of Florida
Kevin Jones
Robert Park
Joe Simmons
Dept. of Materials Science and Engineering
Tim Anderson
Dept. of Chemical Engineering
Peter Zory
Dept. of Electrical Engineering
University of Colorado
Jacques Pankove
Dept. of Electrical Engineering
Columbia University
Gertrude Neumark
Dept. of Materials Science and Engineering
Oregon Graduate Institute of Science and Engineering
Reinhart Engelmann
Dept. of Electrical Engineering

93-31408

93 12 27 101

(I) Molecular Beam Epitaxy Growth of II-VI and III-Nitrides (Robert Park)

(a) Widegap II-VI work

(1) Contacts

In this quarter we adopted the Sony contact scheme (replacing the Brown/Purdue scheme) which is based on a ZnSe/ZnTe hole resonant tunnelling configuration for making contact to p-ZnSe.

We have found the Sony scheme to provide excellent contact to p-ZnSe as evidence by linear I-V characteristics (see Figure I.1 which has 10V and 1mA per division scales) and also by very good specific contact resistance values. Jim DePuydt at the 3M Company has performed transmission line measurements on our samples and reports specific contact resistance values in the $10^{-2}\ \Omega\,cm^2$ range which is comparable to the lowest values reported in the literature.

We have also used the Sony contact scheme to perform Hall-effect measurements on p-type ZnSe:N epilayers by growing four isolated mesas in-situ to act as contact pads following the growth of the p-type material (the mesas comprised the Sony contact scheme). Hall-effect measurements have revealed room temperature free-hole concentrations and hole mobilities to be around $3 \times 10^{17}\ cm^{-3}$ and $20\ cm^2\ V^{-1}s^{-1}$, respectively in our "best" material. We have also performed variable temperature Hall-effect measurements and the data obtained from one sample is shown in Figure I.2. Again, these data are comparable to the best reported in the literature.

(2) Green LED devices

We have also used the Sony contact scheme on our green LED structures which we reported on in the previous quarterly report. Modifications have also been made to the MQW active region of these devices. A schematic of the structure, which only involves Te (in addition to Zn and Se), is illustrated in Figure I.3.

Jim DePuydt at the 3M Company has performed external quantum efficiency and lifetime measurements on our devices and reports excellent data. External quantum efficiencies are around 10^{-3} and the time to half-intensity is greater than one hour (which is better than typically seen).

(b) GaN work

We have further optimized the growth of cubic-GaN on β-SiC coated Si substrates by optimizing the nitrogen rf plasma discharge source operating conditions.

Background free-electron concentrations in unintentionally-doped cubic-GaN films have been reduced from around $10^{19}\ cm^{-3}$ to the $10^{17}\ cm^{-3}$ range. Hall-effect measurements were performed using In contacts.

We have also intentionally-doped cubic-GaN films with Si and have achieved free-electron concentrations in the $10^{20}\ cm^{-3}$ range.

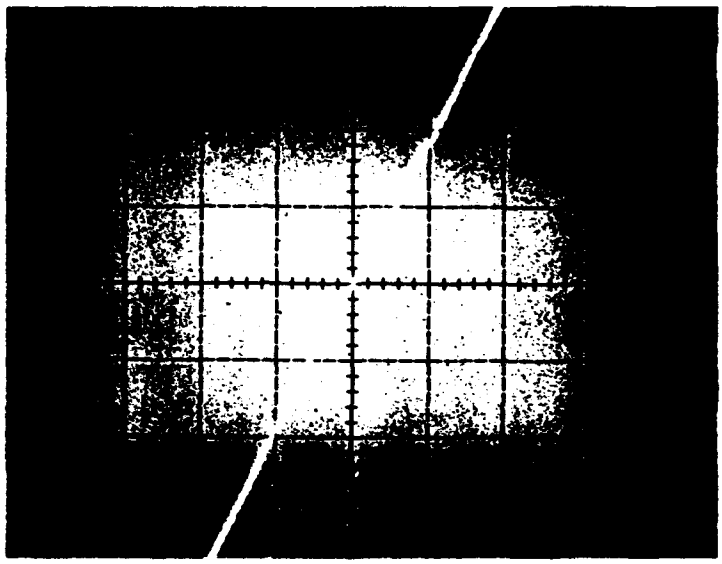

10V/div.;1mA/div

Figure I.1.

Temperature Dependent Hole Mobility and Concentration of p-ZnSe

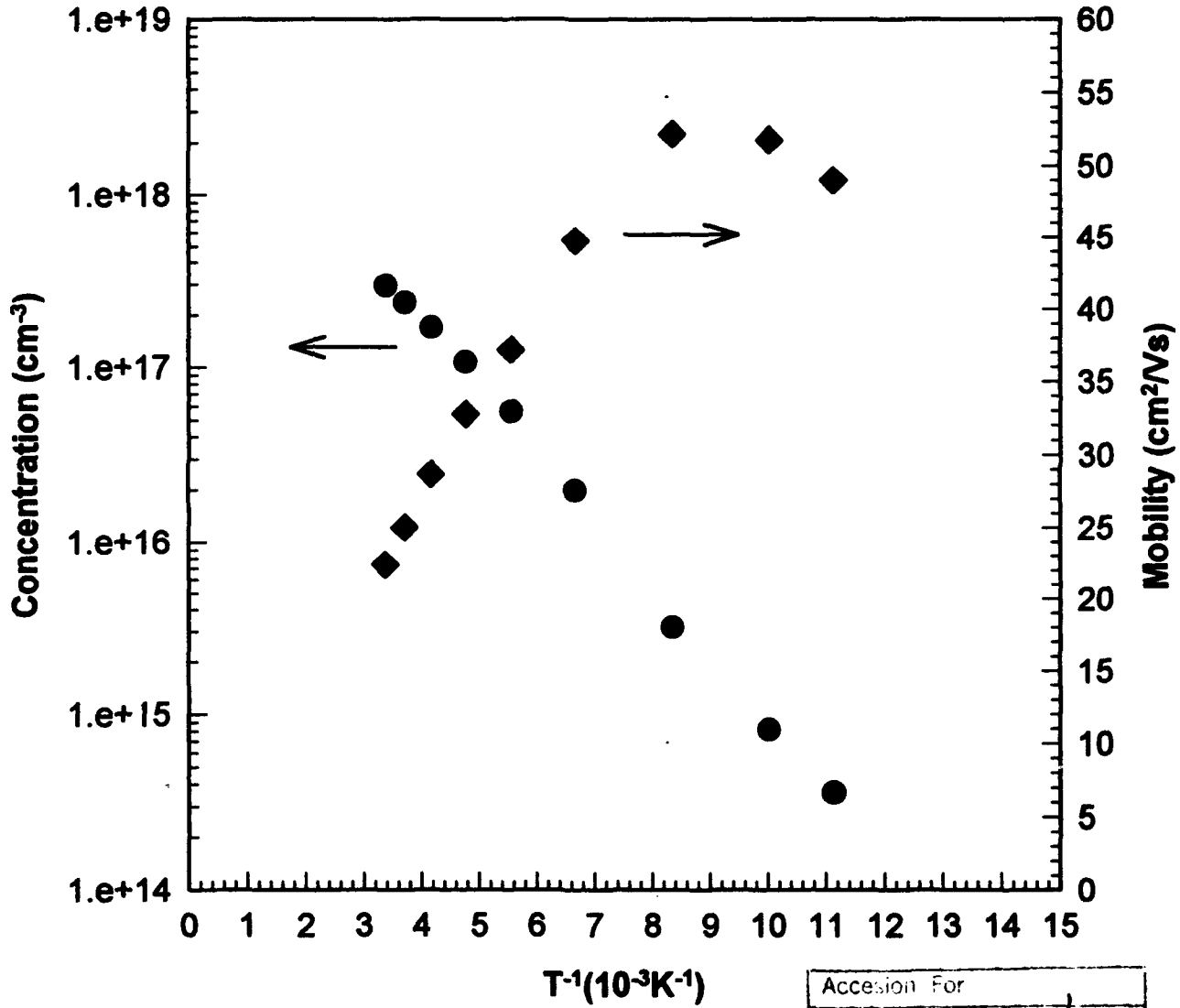

Figure I.2.

DTIC QUALITY INSPECTED 5

Accesion For
NTIS CRA&I
DTIC TAB
Unannounced
Justification
By A 269578
Distribution/
Availability Codes
Dist | Avail and/or Special
A-1

Multiple quantum well diode structure

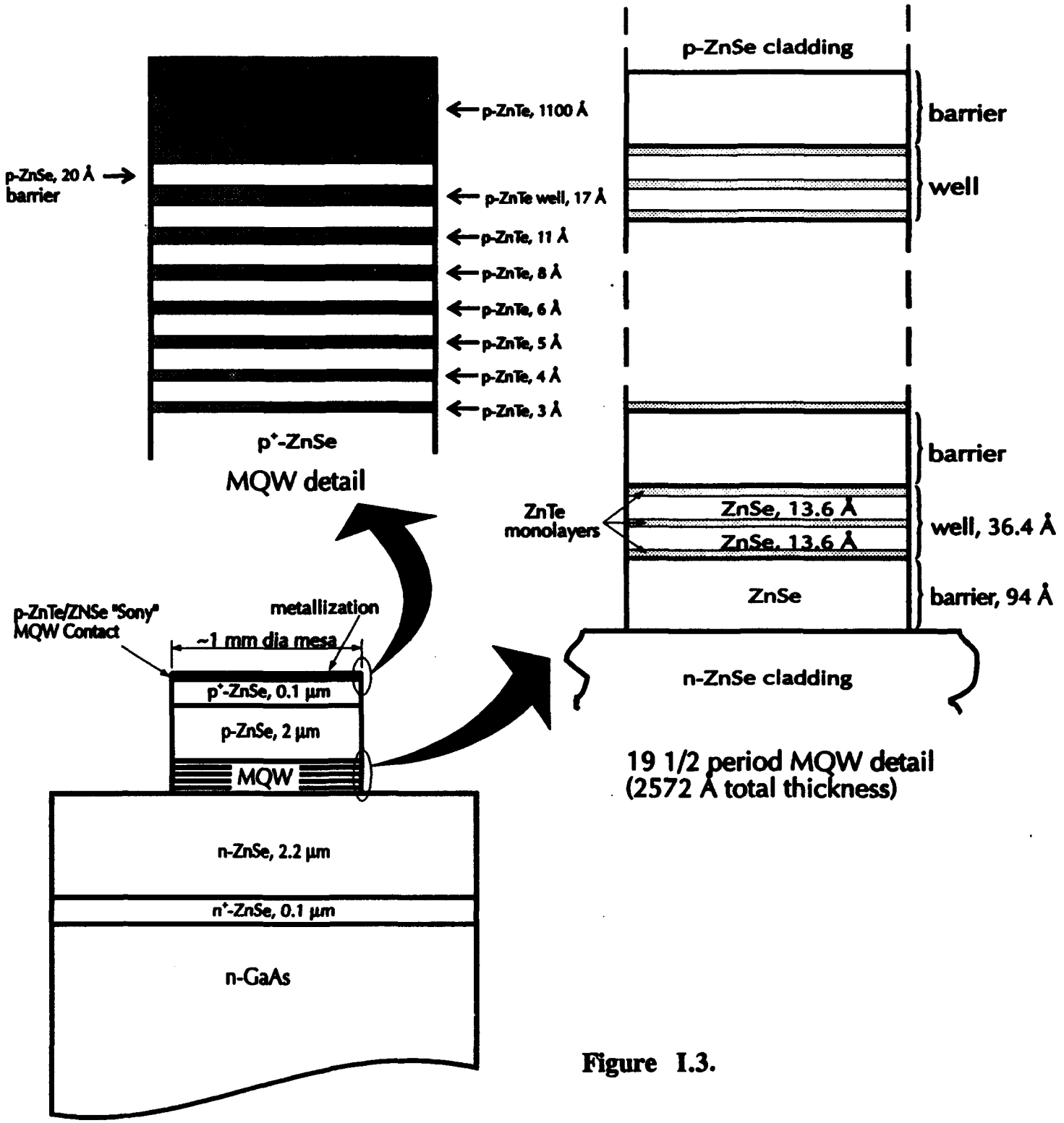

Figure I.3.

(II) Ohmic Contact Formation (Paul Holloway)

Results from the study of Au and Ag contacts on p-type ZnSe were presented at the 40th Annual National Symposium of the American Vacuum Society. The Au and Ag contacts were deposited on p-type ZnSe by DC planar magnetron sputtering. The Au samples were heat treated at temperatures (T) of 150, 200, 300, 350, and 400°C for times (t) of 15, 30, 45, 60, and 90 minutes. I-V results obtained using a Tektronix 177 curve tracer indicate that the reverse bias breakdown voltage of the Au contacts was reduced by heat treatments at $T \geq 350°C$. A minimum reverse bias breakdown voltage of ~ 3 V was obtained for $T = 350°C$ and $t = 15$ minutes. Secondary ion mass spectrometry (SIMS) and scanning Auger depth profiling (SADP) both indicated that Au diffused into the near-surface region of the ZnSe, but no compounds formed during heat treatment. The Ag contacts were heat treated at temperatures of 150, 200, and 300°C for times of 15, 30, 45, 60, and 90 minutes. These samples were found to have a minimum reverse bias breakdown voltage of ~ 2.3V following heat treatment at $T = 150°C$ and $t = 45$ minutes. Both SIMS and SADP failed to detect any diffusion or compound formation during heat treatment. Unlike the Au samples, the resistance of the Ag contacts was observed to increase for heat treatments at $T \geq 200°C$. Therefore, although the Ag contacts were observed to have a lower reverse bias breakdown voltage, the Au contacts were observed to have better temperature stability.

Other efforts have been directed toward *ex situ* formation of $HgSe_{1-x}S_x$ electrical contacts to p-ZnSe. The approach used to form these contacts is a modification of our process of capping p-ZnSe with Se and subsequently reacting the Se cap with Hg vapor to form HgSe. Two methods of introducing S into this process have been investigated. In the first method, S was evaporated onto the Se cap prior to reaction with the Hg vapor. In the second method, the sample was simultaneously exposed to both Hg and S vapor. As in the formation of HgSe, the Hg vapor is carried into a reaction vessel by entrainment in a N_2 gas stream. The S vapor was generated by placing a crucible of S in the reaction vessel with the sample. The sample is then heated in the presence of the Hg and S vapor to facilitate the incorporation of both elements into the Se capping layer. Scanning Auger depth profiling indicates that small amounts of S have been incorporated in the resulting films using both methods. Initial I-V results from these samples indicate that incorporation of S significantly increased the current densities of the contacts as compared to HgSe contacts. The I-V data for samples with 1 mm diameter contacts formed by simultaneous exposure to Hg and S vapor are shown in Figure II.1. During reaction, the Hg was heated to 100°C and the sample and S were heated to 150°C for 15 minutes. A layer of Au was sputter deposited on the contacts and heat treated at 200°C for 15 minutes to insure good electrical conduction between the HgSeS contacts and the electrical probes. The current density for these contacts at 5 V was 0.182 A/cm^2.

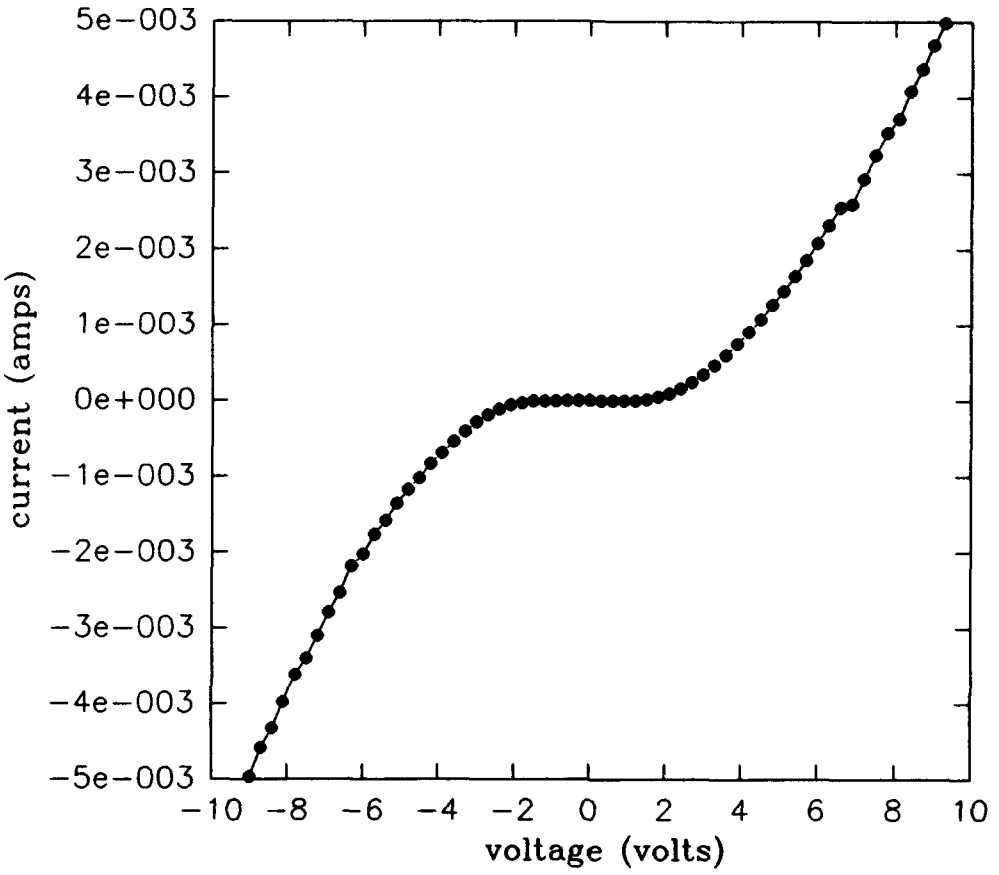

Figure II.1: **Current vs. voltage for Au/HgSeS contacts on p-ZnSe.**

(III) Strain in II-VI epilayers (Kevin Jones)

The research has continued to investigate the strain state and coefficient of thermal expansion (CTE) of the II-VI hetero-epitaxial layers using high resolution x-ray diffractometer (HRXRD). A sample heating stage has been installed as the HRXRD and a peak temperature up to 300°C for at least 2 hours can be obtained. We are now able to get coefficient of thermal expansion and induced strain due to the difference in CTE's for epitaxial layers between room temperature and 300°C which is typical for growth by MBE of II-VI compound semiconductors. For improvement, reducing the sample temperature fluctuation and acquiring a stable glue for use at a high temperature are in progress.

Coefficients of thermal expansion for ZnSe/GaAs and ZnSSe/GaAs epilayers have been measured using HRXRD, and the valves perpendicular to the surface are shown in Figure III.1. These values of CTE are calculated from the lattice constants which are determined by taking (004) rocking curves at temperatures between 25 and 250°C. CTE's for the perpendicular direction are larger than the previous reported values because there is a biaxial compressive strain at the interface and thus most of thermal expansion is accommodated in the perpendicular rather than in the parallel direction. Lattice mismatch for the pseudomorphic ZnSSe/GaAS epilayer has been measured by taking asymmetric (115) diffraction at both room and the growth temperature (250°C). The data are shown in the table below. The results show that the degree of lattice distortion is higher at the growth temperature. It is, however, desirable for the epilayer to have a small distortion at the growth temperature to reduce the induced strain caused by the CTE difference and cooling.

Pseudomorphic ZnSSe/GaAs sample	Lattice mismatch (ppm)	
	Perpendicular	Parallel direction
Room Temperature	225	11
Growth temperature	1,186	5

(IV) Electrical and Optical Characterization (Joe Simmons)

1. Donor and acceptor concentrations for n-ZnSe:

Calculations to model the temperature dependence of six n-ZnSe Cl-doped samples prepared by MBE at the University of Florida were completed. The calculations covered samples with donor concentrations varying from $2x10^{16}$ to $2x10^{19}$ cm^{-3}. The calculations modeled the temperature dependence of the free carrier concentration and mobility. Results showed excellent fitting of the data by the modeled equations. The model and results are being prepared as two journal articles. Briefly, the fits show that the donor levels span

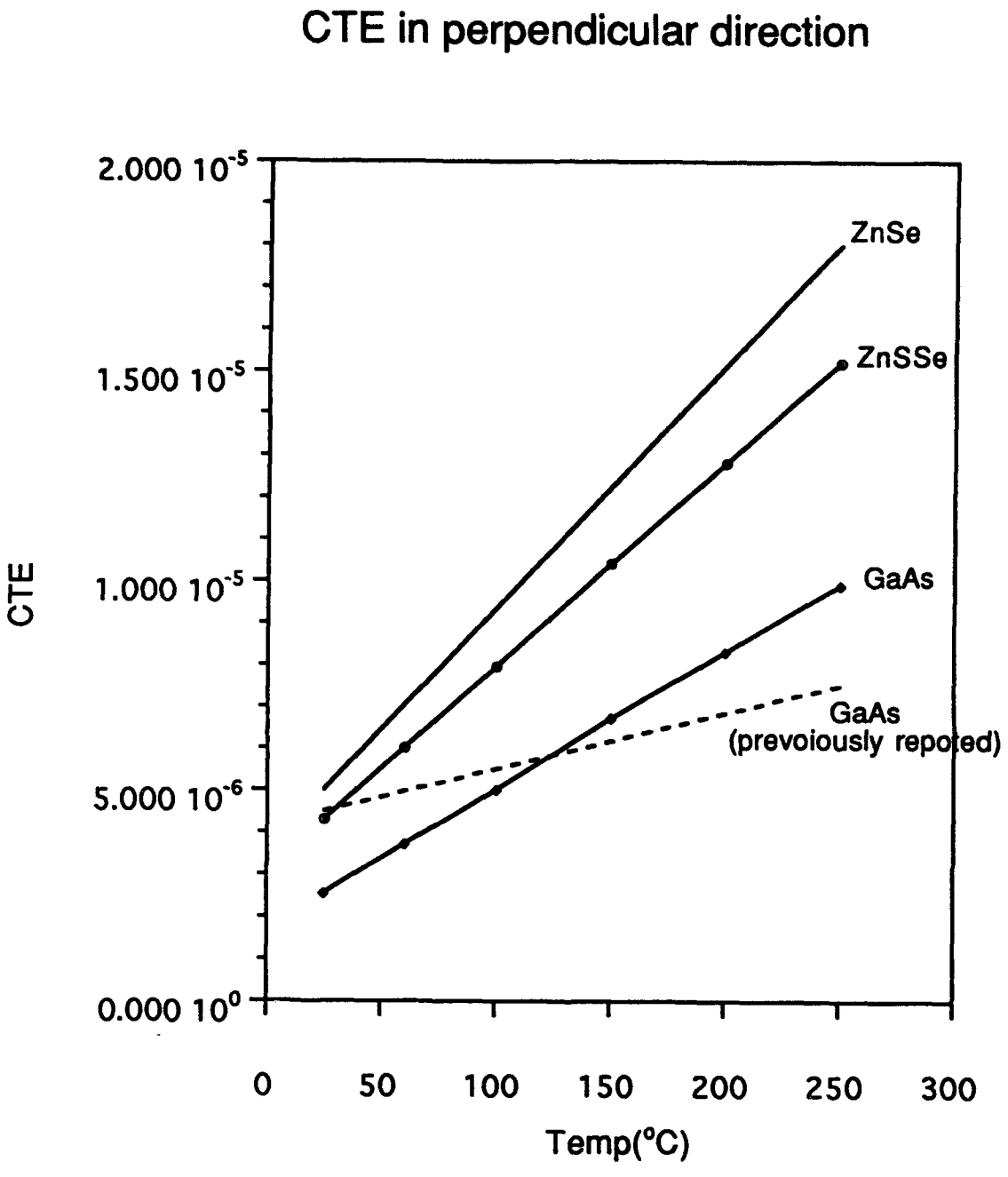
CTE in perpendicular direction
2.000 10-5
1.500 10-5
1.000 10-5
5.000 10-6
0.000 10^0
CTE
ZnSe
ZnSSe
GaAs
GaAs
(prevoiously repoted)
0
50
100
150
200
250
300
Temp(°C)

Figure III.1.

results also give: donor level, acceptor levels, free carrier mobility, donor ionization energy, and hopping conduction mobility. It should be pointed out that this is the first calculation of free carrier density and mobility covering such a wide range of donor levels for any semiconductor.

An example of the use of such calculations is found in the study of compensation. The compensating acceptor concentration can be well established in the mobility calculations. Attached is a graph (Figure IV.1) of the acceptor concentration as a function of the donor concentration. The plot shows a power-law relationship between donor and acceptors. This is demonstrated through the solid line in the graph with an exponent of 1.14. Also shown in the graph as a dashed line is a linear relationship between donor and acceptor concentrations, with the compensation ratio remaining near 24%. Note that this relationship, while closely describing the behavior of the n-doped ZnSe, underestimates the acceptor concentrations at high donor levels. This indicates that the compensation ratio actually increases with increasing donor level, reaching a maximum of 50% for the $2x10^{19}$ cm^{-3} donor concentration. More examples will follow later.

2. Routine measurement of PL to determine thin film and device quality:

Measurements have been conducted on p-ZnSe and GaN films. The resolution afforded by the use of a closed cycle refrigerator was limited by the temperature achieved at the sample, which rarely decreased below 12K, despite a thermometer reading of 9K. We have modified the cooling expander to obtain lower temperatures at the sample. This modification is complete and will be tested in the next quarter.

3. Time resolved studies of photo-excited carrier behavior and relaxation:

Instrumentation for conducting time resolved photoluminescence and pump probe measurements on prepared samples has been delivered and preliminary tests indicate that we may begin acquiring reliable data of photo-excited carrier lifetimes in the next quarter. Our plans are to first test excitonic behavior in ZnSe single quantum wells.

(V) MOCVD Growth (Tim Anderson)

Research efforts have continued on the growth of the alternative pseudoternary material system $Zn_xCd_yMg_{1-x-y}S$ for visible light emitters. This material system has several advantages. First, lattice matching to high quality GaAs substrates is possible over a large range of bandgap energy. Additionally, the compositional degrees of freedom exist on the group II sub-lattice. Since MOCVD growth is generally mass transfer limited in the group II species, the distribution coefficient is near unity and control of the solid solution composition is easier. Also, this material system contains S as the only group VI element, thus avoiding the toxicity issues associated with Se precursors. Unfortunately, very little research has been devoted to the growth of this material system.

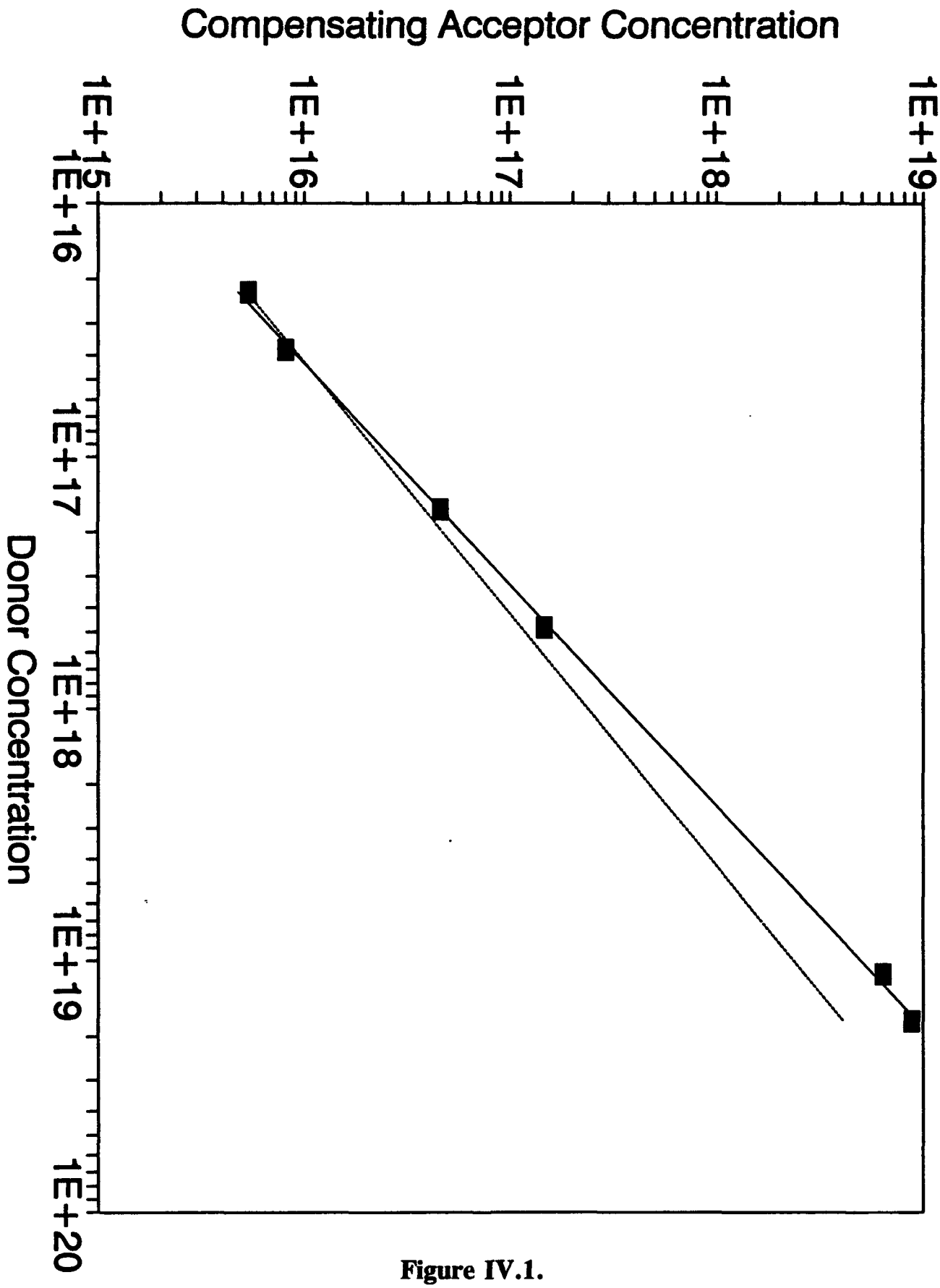
Compensating Acceptor Concentration
1E+15
1E+16
1E+17
1E+18
1E+19
Donor Concentration
1E+16
1E+17
1E+18
1E+19
1E+20

Figure IV.1.

Previous work has focused on the growth of $Zn_xCd_{1-x}S$ from DEZn, DMCd, and H_2S. We have demonstrated the ability to grow epitaxial material that is lattice-matched to GaAs (x_{Zn} @ 0.45). The material is cubic and the lattice parameter and bandgap energy have been determined as a function of alloy composition. Importantly, the low temperature PL spectra indicate that the material is usually free of deep levels. The structural quality of the films, as measured by HRXRD, has been the focus of recent studies. The growth temperature and II/VI inlet molar ratio were varied for the growth of films near the lattice-matched composition. As a result of these studies, we were able to reduce the FWHM of the (400) reflection from the previously reported value of 2000 arc-sec to 900 arc-sec. Although this is the lowest FWHM value reported for growth using this precursor combination, the structural quality needs to be improved further.

One possible reason for the large XRD FWHM value is compositional grading in the film. The results of a SIMS profile, however, indicate excellent compositional uniformity in the growth direction. From XTEM micrographs and electron diffraction results, the XRD FWHM results correlate with the density of stacking faults along the (111) planes. The stacking fault density is high ($\sim 10^{10}$ cm^{-2}) and a Zn-rich ($x_{Zn} = 0.45$) composition relative to the room temperature lattice matching condition (x_{Zn} @ 0.42) has produced the best result. We have begun a series of experiments to reduce the stacking fault density. In these experiments, the GaAs substrate orientation will be varied (0, 2, 10 degrees toward the nearest <110>directions for (111)A and (111)B). In addition, the density of stacking faults has been shown to be sensitive to the growth rate (i.e., group II partial pressure) in other material systems. This will also be investigated for the ZnCdMgS system.

In related work, the Gibbs energy of formation of ZnSe is being measured as a function of temperature by a solid state electrochemical technique using yittria stabilized zirconia as the solid electrolyte. This information will be useful in predictions of dopant solubilities. DH samples consisting of lattice-matched ZnCdS and a ZnCdSe active layer have been grown on GaAs. These samples have been given to Peter Zory for optical pumping experiments. Finally, the homogeneous thermal decomposition kinetics of the Zn and Cd precursors are being studied in an impinging jet reactor by gas phase Raman spectroscopy.

(VI) Development of Diode Lasers (Peter Zory)

A. Photopumping

Room temperature photopumping experiments using the 337 nm pulsed nitrogen laser are continuing with MBE-grown GaN samples provided by Robert Park's group and MOCVD-grown CdZnS samples provided by Tim Anderson's group. In order to improve our ability to get carriers deeper into the material to avoid surface recombination effects, we have reactivated the dye laser and are currently calibrating the system with "deep-blue" dyes.

B. Diode Pumping

We have processed a new piece of single quantum well material provided by 3M and demonstrated laser action at 100K (see attached near-threshold spectrum - Figure VI.1). Experiments are continuing with this material to see if we can clarify the role of excitons in generating optical gain. We have also processed a novel ZnTe monolayer multi-quantum well sample with a pseudoternary capping system provided by Dr. Park's group (see section I in previous quarterly report). Room temperature electroluminescence was measured at 519 nm. The differential resistance for 100μm stripe by 1500μm long devices was measured to be about 20 ohms in the 15 A/cm^2 current density regime. New wafers with an improved layer structure are now being processed.

C. Diode Laser Modeling

The paper, "Temperature dependence of threshold current density in CdZnSe single quantum well lasers" was presented by student Y.S. Park at the IEEE/LEOS Annual Meeting in San Jose, California on November 16. Cai and Engelmann have shown that their relatively simple model is in good agreement with the more complex, valence band mixing model used in the University of Florida (UF) paper (see Oregon Graduate Institute Report). The UF model has been used to make some predictions which we are hoping to verify by experiment (see section B above).

(VII) Theoretical Calculations of Dopants in ZnSe (Gertrude Neumark)

As mentioned in the previous progress report, it seems likely that if MBE growth is quasi-equilibrium, one cannot avoid self-compensation. Therefore, we are investigating this point. The thesis that such growth is quasi-equilibrium is strongly supported by work of Turco and Tamargo [J. Appl.Phys. 66 (4), 1695 (1989)], who show that this approach can explain the dependence of growth rate on temperature and on the ratio of Se to Zn pressure.

As also mentioned in the previous report, a vital parameter for determining whether quasi-equilibrium holds is the surface diffusion rate. We have found a literature value, by Gaines et al. [J. Vac.Sci.Technol. B, 10 (2), 918 (1992)], of a diffusion length of 40 Å at the usual growth temperatures. This seems rather low for quasi-equilibrium, and is thus in disagreement with the conclusions of Turco and Tamargo. Further analysis has shown that the method for determining the diffusion length used by Gaines et al will lead to low values, by two orders of magnitude in the case of GaAs [Hata et al., Appl.Phys.Lett. 56 (25), 2542 (1990). These authors attribute the discrepancy to the possibility that migrating atoms which cross a growth island go through the step and do not stick to it. On this basis, the surface diffusion length is a quite complicated quantity, and evaluation would require not only the rate of motion over the surface, but also the capture rate at the steps. These quantities do not appear to be available for ZnSe, and we are currently uncertain as to whether we can use prior GaAs theories which require such parameters. We plan to investigate whether the

Spectrum of $Cd_{.2}Zn_{.8}Se$ 100Å SQW Diode Laser Near Threshold

T=100K

W=30μm

L=250μm

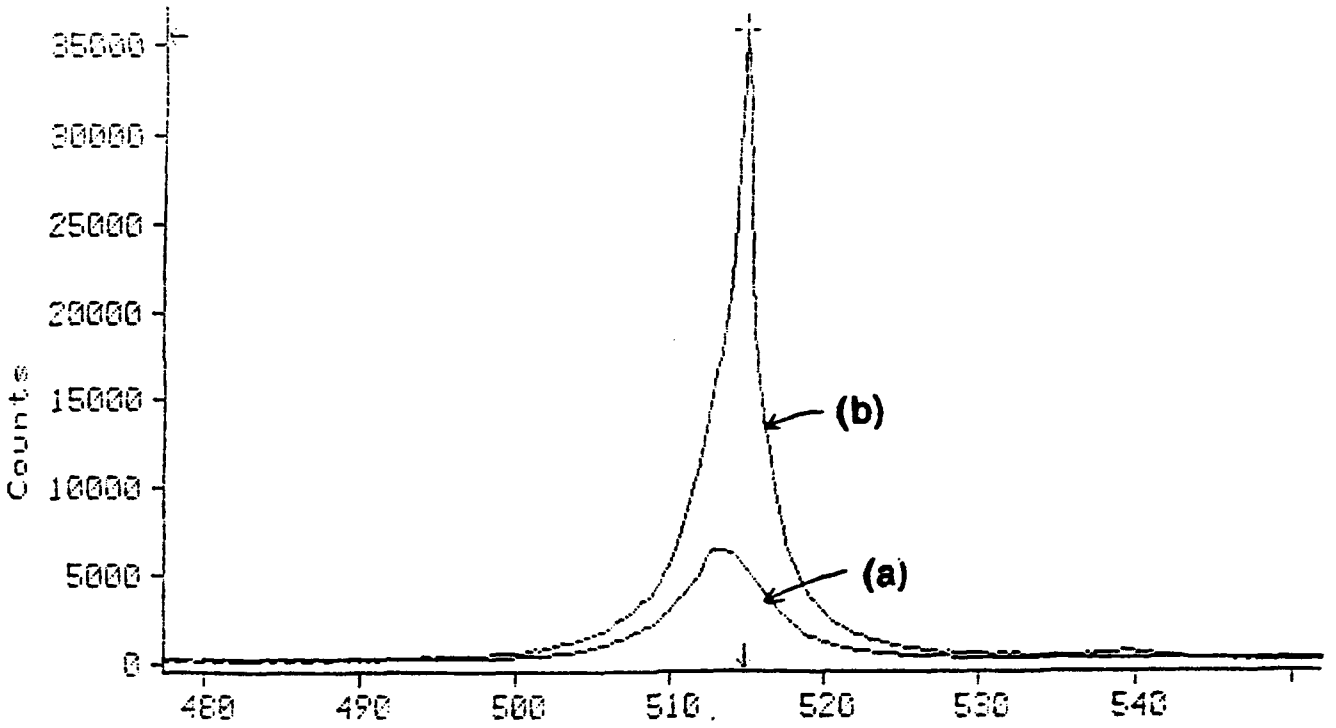

(a) i=200mA

(b) i=300mA

3M / University of Florida

Figure VI.1.

question of quasi-equilibrium can be quantified, in the absence of values for these parameters, by alternate approaches (perhaps from functional dependencies of growth on temperature and pressure).

In summary, based on the results of Turco and Tamargo and of those of Hata et al., it appears likely that, under usual growth conditions, MBE growth of ZnSe is quasi-equilibrium. We plan to investigate whether a more quantitative treatment is feasible, given difficulties of obtaining information on requisite empirical input parameters.

(VIII) GaN part of DARPA-URI Project on Wide Band-gap Semiconductors for Short Wavelength Emitters (J.I. Pankove)

Our objective is to grow pn junctions in GaN that will be the basis for short wavelength emitters and lasers.

In the past quarter, the quality of GaN films was improved further. The runs in the first system (a low-pressure vertical MOCVD system) concentrated on p-type doping using ammonia from Salkatronix. A tank of Matheson high purity hydrogen was installed both to carry the TEG and Cp_2Mg, as well as for extra dilution. Many Mg-doped films are insulating. Some slightly Mg-doped samples remain n-type as determined by thermoelectric measurements. The mirror-like films grown in the first system exhibit strong edge luminescence at 3.45 eV (see Figure VIII.1), indicating fewer defect centers in the band-gap region of GaN. As a comparison, the intensity of the edge luminescence for the films grown in this system was usually less than one tenth of the intensity of the yellow peak. The much more intense edge luminescence peak may result from extra hydrogen dilution. The shoulder around 3.2 eV may be due to Mg-doping. The shoulder around 3.66 eV is a mystery, probably due to an interface layer of AlGaN. The highest electron mobility of the doped films is about 38 $cm^2/Vsec$.

Dr. Balu Pathangey at the University of Florida made SIMS measurements on our Mg-doped films, and verified Mg incorporation. In addition, the measurement showed a reasonably sharp spatial transition between the undoped and doped regions.

In the second deposition system (a *horizontal* cold-wall MOCVD system), we are evaluating the effect of different supersonic nozzles on the quality of the GaN deposition. Using the first nozzle, films with dominant edge luminescence, as reported last quarter, were deposited. An almost-horizontal nozzle was installed in October to improve the uniformity of the films. The deposition rate using this nozzle is very small, only 100 Å/hour. The vertical distance between the nozzle and horizontal substrate was about 1 cm, which might be too large. A third quartz nozzle with a small angle and a closer vertical distance to the substrate was made and installed last month. Recent runs only give black and insulating deposited material. A new substrate holder was also made and used during the last quarter.

Pankove lab.

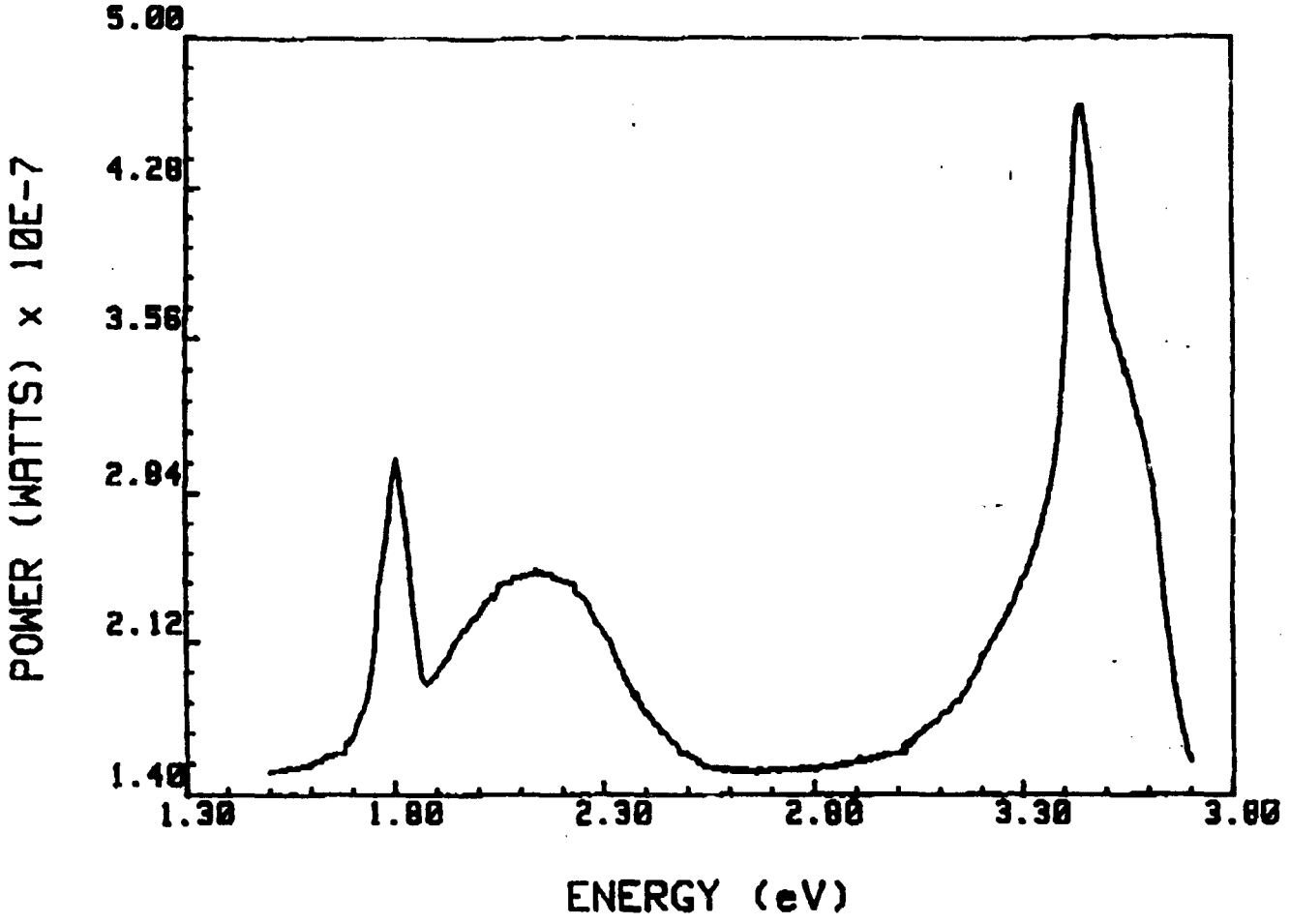

Figure VIII.1: **Cathodoluminescence spectrum of a GaN film grown on basal plane sapphire. The peak around 1.8 eV is due to the substrate, and the shoulder around 3.2 eV may arise from Mg-doping.**

(IX) Gain Modeling in II-VI Strained-Layer QW Structures (Reinhart Engelmann)

The structure parameters of ZnCdSe/MgZnSSe SCH SQW diode lasers were optimized for low threshold current density operation by modeling the optical gain based on the electron-hole plasma theory, and the optical confinement factor G in the SCH waveguide. A substantial reduction in threshold current density from about 500 A cm^{-2} in the commonly used laser structure to as low as about 200 A cm^{-2} is predicted.

The structure dependence of the optical confinement factor Γ [*], gain, and threshold current density J_{th} for the separate-confinement-heterostructure (SCH) quantum well (QW) diode lasers of the MgZnSSe system has been modeled. We have chosen a compressively strained $Cd_{0.2}Zn_{0.8}Se$ SQW which provides a room-temperature (RT) lasing wavelength of about 500 nm. The (Mg) ZnSSe barrier and cladding layers are lattice matched to the GaAs substrate. The composition, band-gap energy and refractive index of the GaAs lattice-matched MgZnSSe alloys are listed in Table 1. The refractive index data are estimated from Ref. [1]. The band alignment rules are similar to the ones used by Park and Zory [3].

A simplified approach based on the electron-hole plasma theory with constant effective masses as described in the First Annual Report has been used to model the optical gain in the QW. In our Fifth Quarterly Report we presented modeling results of threshold current density vs. temperature using a simple 2D density-of-states model. Additional refinements of the theory, such as QW anisotropy and the intraband relaxation effect on the optical gain spectra, have now been included to estimate threshold current density. The intraband relaxation was taken into account assuming Lorentzian broadening with a fixed intraband relaxation time T_s. The influence of carrier spill-over into the barrier on the injected current as analyzed in our Fifth Quarterly Report was also taken into account. The peak values of the optical gain spectra vs. total injected current density were then calculated for different temperatures allowing for the temperature dependence of the band gap. Using these data, the threshold current density was determined from the threshold gain as estimated from the total cavity loss (23 cm^{-1} assuming 1 mm long cavity) and the confinement factor Γ. Modeling results agree well with experimental J_{th} data versus temperature [2] when choosing an intraband relaxation time $T_s = 0.1$ ps, a value somewhat larger than reported for a more accurate model [3] but consistent with GaAs data (Figure IX.1). Based on this approach the optimized structure parameters for low threshold current density operation have been obtained.

First, we only consider the influence of the barrier layer. The QW layer thickness L_{qw} is chosen as 6.5 nm. For the commonly used laser structure with a $Cd_{0.2}Zn_{0.8}Se$ SQW, a $ZnS_{0.06}Se_{0.94}$ barrier (composition A) and a $Mg_{0.1}Zn_{0.9}S_{0.14}Se_{0.86}$ cladding layer (composition C) [2], the barrier size L_{ba} on each side of the QW which provides the maximum Γ is about 100 nm (Figure IX.2) as compared with 250 nm used in Ref. [2]. Thus, at RT J_{th} could be reduced from 554 to 399 A cm^{-2} just by optimizing the barrier size. However, a $ZnS_{0.06}Se_{0.94}$ barrier still provides only a relatively small band gap difference to the strained $Cd_{0.2}Zn_{0.8}Se$ QW, leading especially in the valence band to an insufficient band offset for preventing carrier spill-over into the barrier. To eliminate such spill-over, we propose an improved configuration by using a $Mg_{0.05}Zn_{0.95}S_{0.1}Se_{0.9}$ layer (composition B) with a larger band gap $E_g = 2.79$ eV as barrier material (see also First Annual Report). This reduces the

optimized J_{th} value to 376 A cm^{-2}. For better optical confinement, the cladding layer requires increased Mg content as summarized in Table 2. The optimized J_{th} at RT for a $Mg_{0.5}Zn_{0.5}S_{0.48}Se_{0.2}$ cladding layer (composition I) is predicted to be as low as 224 A cm^{-2}.

Second, we are studying the J_{th} dependence on L_{qw}. In the range of 2.5 nm - 10 nm, the J_{th} dependence on L_{qw} for one particular structures is plotted in the Figure IX.3. Initial investigation suggest that relative thin QW layer should be used in these devices (L_{qw} = 4.5 nm gives the lowest J_{th} in Figure IX.3), as compared with the III-V devices (L_{qw} usually larger than 5.0 nm). This is due to the relatively large effective mass in II-VI materials.

In conclusion, a substantial reduction in threshold current density from about 500 A cm^{-2} in the commonly used laser structure to as low as about 200 A cm^{-2} is predicted by increasing the Mg content in both barrier and cladding via optimizing the structure parameters of ZnCdSe/MgZnSSe SCH SQW diode lasers.

Future Plans

In the future, more calculations will be performed to establish the optimized QW size L_{qw} for different SCH structures. The role of the temperature dependence of the scattering time T_s and confinement factor Γ will also be considered. A more comprehensive model, with particular emphasis to properly model the carrier injection mechanism into the various regions of the SCH structure, will be studied in cooperation with P. Zory of the University of Florida and P. Mensz of Philips Lab.

References

[*] Computer program for waveguide modeling by courtesy of Gary Evans, Southern Methodist University.

[1] M. Ukita, H. Okuyama, M. Ozawa, A. Ishibashi, K. Akimoto and Y. Mori, Appl. Phys. Lett. 63 (15), 2082, 1993.

[2] J. Gaines, R. Drenten, K. Haberern, T. Marshall, P. Mensz, and J. Petruzello, Appl. Phys. Lett. 62 (20), 2462, 1993.

[3] Y.S. Park and P.S. Zory, IEEE/LEOS Annual Meeting in San Jose, CA, Nov. 1993.

Alloy Symbol	$Mg_xZn_{1-x}S_ySe_{1-y}$		E_g (eV) @ RT	Refractive Index n @500 nm
	x	y		
A	0	0.06	2.73	2.7
B	0.05	0.10	2.79	2.67
C	0.10	0.14	2.85	2.62
D	0.15	0.19	2.92	2.56
E	0.25	0.27	3.05	2.46
F	0.30	0.31	3.12	2.40
G	0.50	0.48	3.41	2.17

Table 1: MgZnSSe alloys composition with lattice matched to GaAs and calculated room temperature band gap and refractive index at 500 nm.

Barrier/ Cladding	Difference of Refractive Index Δn	Barrier Length L_{ba} (nm)	Opt. Confinement factor Γ	Threshold Gain (cm^{-1})	J_{th} (A cm^{-2})
A/C	0.08	250 (un opt.)	0.017	1364	554
A/C	0.08	100 (opt.)	0.022	1056	399
B/C	0.05	125 (opt.)	0.019	1221	376
B/D	0.11	75 (opt.)	0.027	860	296
B/E	0.21	65 (opt.)	0.036	644	257
B/F	0.27	50 (opt.)	0.040	580	246
B/G	0.50	50 (opt.)	0.052	446	224

Table 2: Optical confinement factor Γ, threshold gain and threshold current density J_{th} of the SCH diode laser structures with 6.5 nm $Cd_{0.2}Zn_{0.8}Se$ strained SQW, and different combinations of MgZnSSe layers as the barriers and claddings.

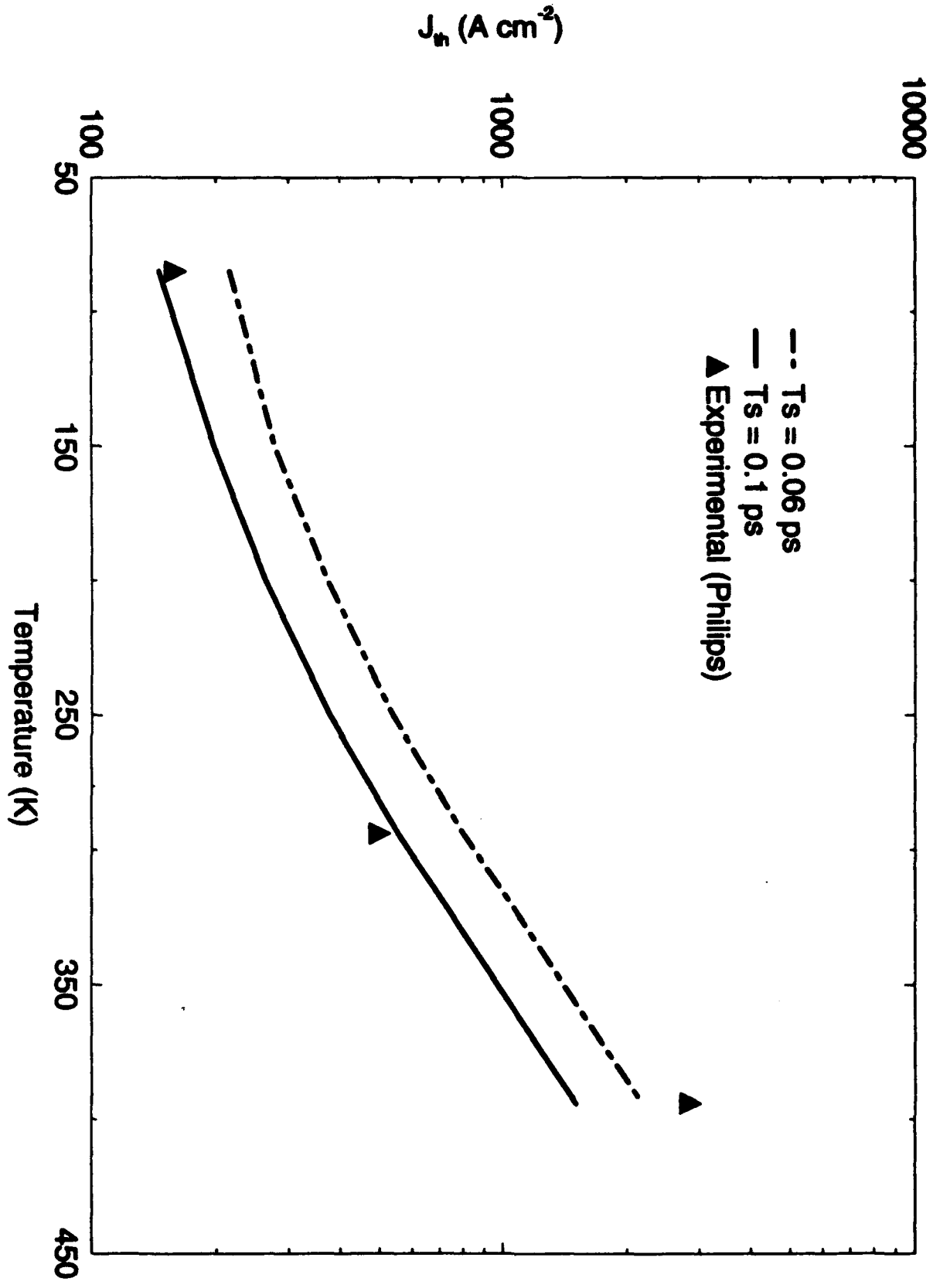
J_{th} (A cm^{-2})
100
1000
10000
50
150
250
350
450
Temperature (K)
Ts = 0.06 ps
Ts = 0.1 ps
Experimental (Philips)

Figure IX.1.

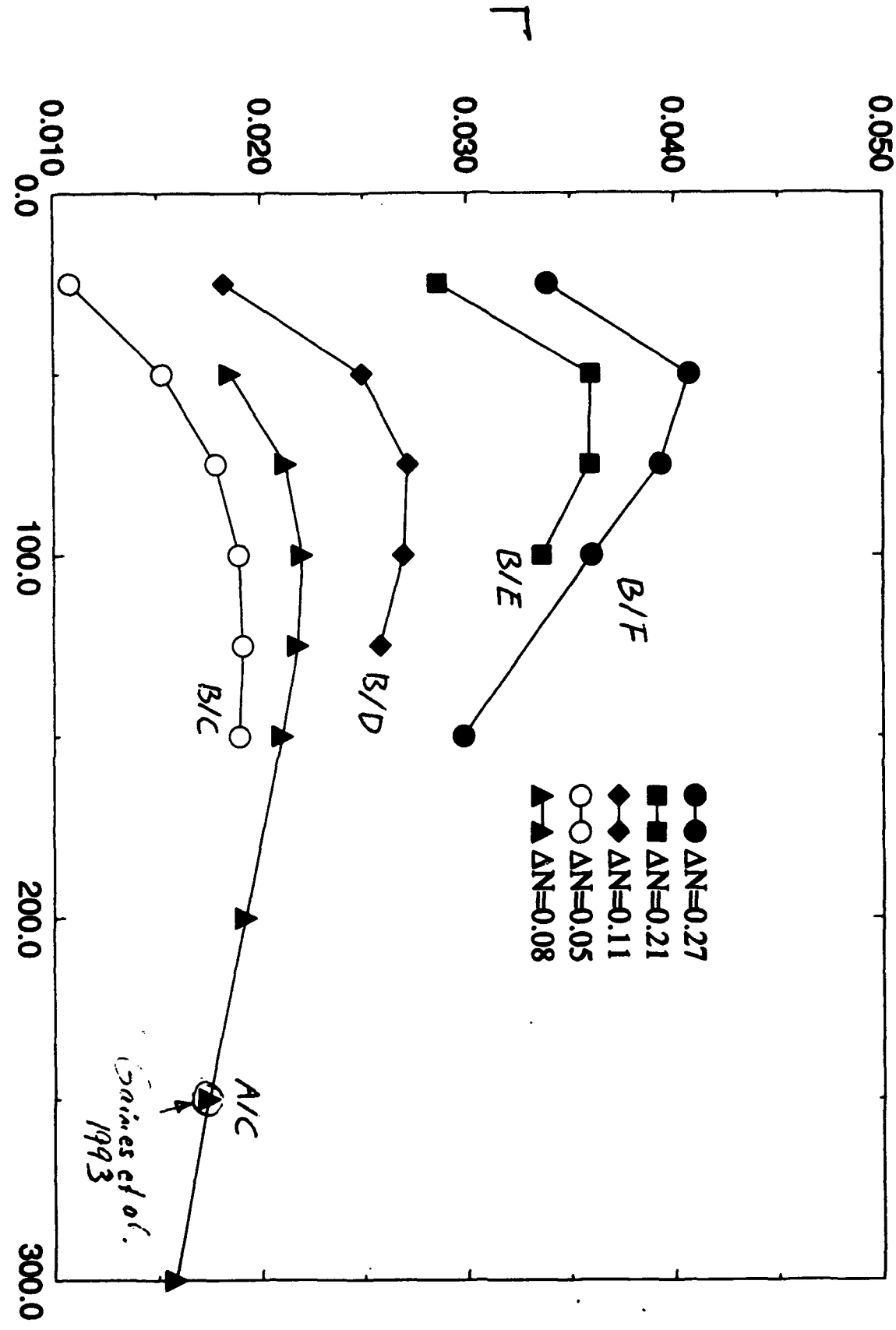
Γ
0.050
0.040
0.030
0.020
0.010
0.0
100.0
200.0
300.0
ΔN=0.27
ΔN=0.21
ΔN=0.11
ΔN=0.05
ΔN=0.08
B/E
B/F
B/D
B/C
A/C
Daines et al. 1993
L_{ba} (nm)

Figure IX.2.

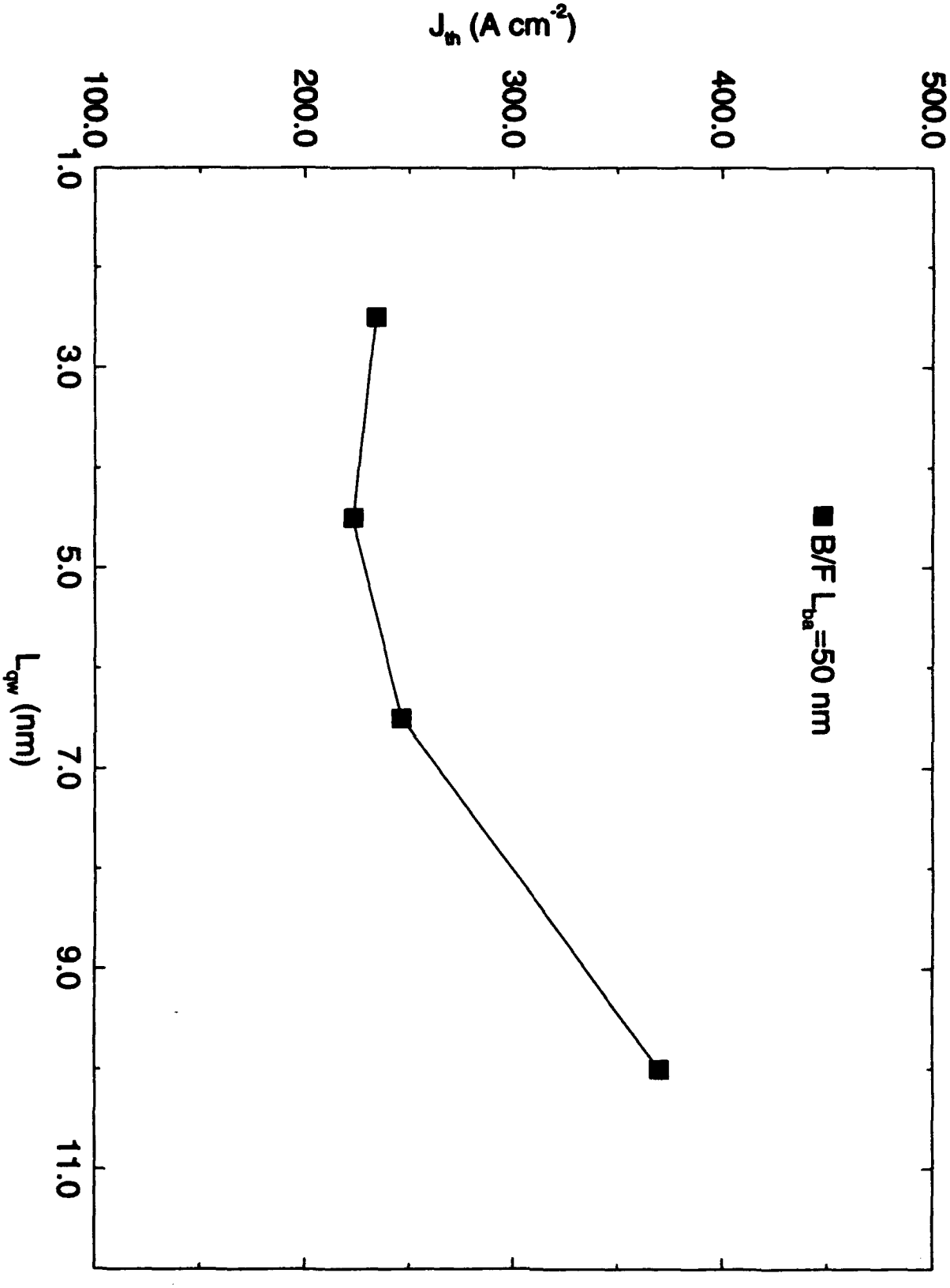
J_th (A cm^-2)
100.0
200.0
300.0
400.0
500.0
1.0
3.0
5.0
7.0
9.0
11.0
L_qw (nm)
B/F L_ba=50 nm

Figure IX.3.

Presentations this quarter

- R.M. Park, "p-type ZnSe:N grown by MBE: evidence of non-radiative recombination centers in moderately to heavily-doped material," Sixth International Conference on II-VI Compounds and Related Opto-electronic Materials, Sept. 13-17, 1993, Newport, RI.

- P. S. Zory, "Blue-Green Diode Laser Overview", IEEE/LEOS Annual Meeting, San Jose, CA, November 15-18, 1993. (Invited)

- Y. S. Park and P. S. Zory, "Temperature Dependence of the Threshold Current Density in CdZnSe Blue-Green Quantum Well Diode Lasers", IEEE/LEOS Annual Meeting, San Jose, CA, November 15-18, 1993.

- P. Zory, "Conclusions reached at the July IEEE/LEOS Topical Meeting Panel Discussion on 'II-VI vs III-V - Which Will Win the Blue-Green Diode Laser Reliability Race'," evening session, II-VI laser Workshop in Ossining, NY on November 8-9, 1993.

- P. Zory, Chair of "Contacts and Degradation" session, II-VI laser Workshop in Ossining, NY on November 8 -9, 1993.

- J.J. Fijol, J. Trexler and P.H. Holloway, "Ohmic contacts to n- and p-type ZnSe," 40th Annual National Symposium of the American Vacuum Society, Orlando, FL, November 15-19, 1993.

- P.H. Holloway, T.J. Kim, V. Fischer, W. Lampert, W. Haas and J. Woodall, "Segregation and regrowth effects in the formation of ohmic contacts on GaAs," 40th Annual National Symposium of the American Vacuum Society, Orlando, FL, November 15-19, 1993.

Papers published during quarter

- H. Liu, A.C. Frenkel, J.G. Kim and R.M. Park, "Growth of zincblende-GaN on β-SiC coated (001) Si by MBE using a rf plasma discharge, nitrogen free-radical source," J. Appl. Phys. (1993) Nov. 15 issue.

Honors :

- Paul Holloway was elected Fellow the the American Vacuum Society in the inaugural class for this membership category. His citation for the award reads: "For his contributions in the areas of surface analysis and materials characterization that have advanced the understanding of the properties of electronic materials, interfaces, contacts and the performance of semiconductor devices."

- Dr. Robert Park received the prestigeous Rank Prize in Optoelectronics for his discovery of the use of nitrogen for p-doping ZnSe. He shared the prize with Hwa Cheng, James M. DePuydt, Michael A. Haase, and Jean Qui of 3M Company. Dr. Park presented the results of their collaborative work to the Royal Society in London on November 30, 1993.

- Mr. Chris Rouleau won the MRS Graduate Student Award at the Fall meeting in Boston, November 29 to December 3, 1993.

Post Doctoral Associates, Graduate Research Assistants, and Undergraduate Research Assistants :

Post Doctoral Associates:

Wafaa Gobba with Dr. Simmons
Chang H. Qiu with Dr. Pankove

Graduate Research Assistants:

Bruce Liu with Dr. Park
Austin Frenkel with Dr. Park
George Kim with Dr. Park
Y.S. Park with Dr. Zory
C.L. Young with Dr. Zory
Igor Kuskovskiy with Dr. Neumark
Li Wang with Dr. Simmons
Y. Cai with Dr. Engelmann
Charles Hoggatt with Dr. Pankove
William A. Melton with Dr. Pankove
John Fijol with Dr. Holloway
Jeff Trexler with Dr. Holloway
Steve Miller with Dr. Holloway
Eric Bretschneider with Dr. Anderson
Joe Cho with Dr. Anderson
J. Kim with Dr. Jones
S. Bharatan with Dr. Jones

Post Doctoral Associates, Graduate Research Assistants, and Undergraduate Research Assistants: **(Continued)**

Undergraduate Research Assistants:

Julie Sauer with Dr. Simmons
Greg Darby with Dr. Park
Bob Covington with Dr. Anderson
Michael Mui with Dr. Anderson
Brendon Cornwell with Dr. Anderson